

# The electron cusp condition and the virial ratio as indicators of basis set quality

Victor M. Rosas-Garcia and T. Daniel Crawford<sup>a)</sup>  
*Department of Chemistry, Virginia Tech, Blacksburg, Virginia 24061*

(Received 1 October 2002; accepted 13 November 2002)

We consider two measures of the quality of one-electron basis sets for quantum-chemical calculations: The electron–electron coalescence curvature and the correlation energy virial ratio. The former is based on the Kato cusp condition that many-electron wave functions must exhibit discontinuous first derivatives with respect to  $r_{12}$  as the coordinates of any two electrons coalesce. The latter is based on a simple modification of the quantum-mechanical virial theorem that makes use of only the correlation contributions to the kinetic and potential energy expectation values. The two measures are tested using coupled cluster wave functions for helium, neon, argon, calcium, and phosphorus atoms and are found to indicate good correlation with the quality of the basis set. These techniques may provide a foundation for the development of reliable basis set diagnostics for a variety of quantum-chemical applications. © 2003 American Institute of Physics.  
[DOI: 10.1063/1.1535440]

## I. INTRODUCTION

One of the most important factors in the design and application of reliable quantum-chemical computations is the selection of a basis set, the group of functions used to parametrize the approximate electronic wave function. For polyatomic molecules, these functions are almost invariably taken to be nucleus-centered one-electron Gaussian orbitals, with different levels of orbital angular momentum ( $s$ ,  $p$ ,  $d$ , etc.), optimized in atomic environments. Within the space described by the basis set, the electronic structure problem may then be solved using a variety of methods, such as Hartree–Fock, perturbation theory,<sup>1</sup> density-functional theory (DFT),<sup>2</sup> or coupled cluster (CC) theory.<sup>3–5</sup>

The development of Gaussian basis sets has a long history, and tremendous strides have been made in the last 15–20 years particularly with the introduction of atomic natural orbital (ANO)<sup>6,7</sup> and correlation-consistent basis sets.<sup>8,9</sup> The ANO basis sets are designed to minimize the losses in both the correlation and reference energies due to the contraction process. As these orbitals generally come from atomic configuration interaction calculations, they are better suited to describe correlation effects than functions derived from self-consistent field (SCF) calculations. The correlation-consistent basis sets, which were devised by Dunning and co-workers,<sup>9</sup> are also optimized using correlated wave functions. In addition, they are designed to include correlation contributions in a balanced fashion, i.e., groups of  $spd$  . . . functions that make similar contributions to the correlation energy are included together.

These new basis sets, in conjunction with extrapolation and focal-point techniques,<sup>10–14</sup> allow estimates of molecular energies at the complete basis set (CBS) limit, where a series of larger and larger basis sets is employed until an acceptable level of convergence is attained. As a result, quantum-

chemical computations of so-called “chemical accuracy” are now common, with properties such as heats of formation determined to within 1.0 kcal/mol of the best experimental measurements.

Unfortunately, such high accuracy is possible only for very small molecules, containing at most a few nonhydrogen atoms. For larger chemical systems, calculations are limited to small basis sets due to the unreasonably steep scaling of quantum-chemical methods with the size of the system. In addition, even for small cases, carefully constructed basis sets may contain serious inadequacies when used to compute properties other than those for which the basis was originally optimized. A recent paper by Wesolowski, Valeev, King, Baranovski, and Schaefer<sup>15</sup> showed how an insufficient  $d$ -angular momentum space in a widely used ANO basis set for calcium led to errors in predictions of the Ca–O bond length of more than 0.25 Å, even at the usually accurate CCSD(T) level of theory (coupled cluster including all single and double excitations plus a perturbative estimate of connected triple excitations).<sup>16</sup> The same basis set led to an error of more than 12 000 cm<sup>-1</sup> in the EOM-CCSD (equation-of-motion CCSD)<sup>17</sup> prediction of the  $^2P \leftarrow ^2S$  excitation energy of Ca<sup>+</sup>. As shown by Wesolowski and co-workers, the addition of a single set of high-exponent  $d$ -type functions corrected these problems, and reduced the errors to only 0.08 Å in the Ca–O bond length and 100 cm<sup>-1</sup> in the Ca<sup>+</sup> excitation energy.

The quality of a given basis set can be understood in terms of its ability either to reproduce results close to experimental values for properties of interest or to reproduce properties of approximate wave functions represented in a complete basis set. Obviously, the ultimate goal is to develop basis sets that provide reliable predictions of observable data, but comparisons to the CBS limit provide a systematic route to diagnosing problems in and improving upon current basis set technology. Several authors have considered basis set di-

<sup>a)</sup>Electronic mail: crawdad@vt.edu

agnostics before. Chong has developed a series of one-electron “completeness profiles” that provide a visual assessment of the quality of the basis for a given angular momentum level. Chong tested these profiles in a number of atomic cases in order to examine the quality of Chipman basis sets for spin-density contributions for Fermi contact calculations.<sup>18,19</sup> Auer and co-workers extended this approach to consider electron correlation effects by defining two-electron completeness projectors,<sup>20</sup> which they used to examine the quality of the Dunning correlation consistent basis sets. This work explores two additional possibilities for measuring the completeness and adequacy of finite basis sets: The electron–electron cusp condition and the quantum-mechanical virial ratio.

## II. ELECTRON COALESCENCE CURVES

In 1957, Kato explained that exact many-electron wave functions must exhibit cusps in regions where the coordinates of any two electrons coalesce.<sup>21</sup> However, for determinantal wave functions this condition is never fully achieved, and, with finite basis sets, such wave functions exhibit minima at values of  $r_{12}=0$ . Nevertheless, as the basis set approaches completeness, the curvature of the correlated wave function around the coalescence point increases, and it is reasonable that this behavior could be used as a diagnostic of the quality of the basis. The development of R12 methods by Kutzelnigg, Klopper and co-workers makes use of the Kato cusp condition by explicit inclusion of linear interelectronic  $r_{12}$  components in correlated wave functions. This method has found great success in recent years within perturbation theory and coupled cluster theory, among others.<sup>22–27</sup>

An analysis of the Kato cusp condition for the wave function is straightforward for two-electron wave functions such as that of He. However, for application of the cusp condition to many-electron systems, we may similarly analyze the two-electron density<sup>28</sup>

$$\Gamma(\mathbf{r}_1, \mathbf{r}_2) = \int |\Psi(\mathbf{r}_1, \mathbf{r}_2, \dots, \mathbf{r}_n)|^2 d\mathbf{r}_3 d\mathbf{r}_4 \dots d\mathbf{r}_n. \quad (1)$$

That is, as the electron coordinates  $\mathbf{r}_1$  and  $\mathbf{r}_2$  coalesce, the exact density,  $\Gamma(\mathbf{r}_1, \mathbf{r}_2)$  exhibits a discontinuous first derivative. For approximate wave functions in finite basis sets, the density instead contains a minimum, which becomes sharper as the basis becomes more complete.

In order to test the use of the Kato cusp condition as an indicator of basis set quality, we have computed the two-electron density using coupled cluster theory truncated at the single- and double-excitation level (CCSD).<sup>29</sup> Coupled cluster includes high levels of dynamic electron correlation and is one of the most reliable quantum-chemical methods.<sup>5</sup> The coupled cluster two-electron density may be written in second-quantized form as<sup>30–34</sup>

$$\Gamma_{pqrs}^{\text{CC}} = \langle 0 | (1 + \hat{\Lambda}) e^{-\hat{T}} \{ a_p^\dagger a_q^\dagger a_r a_s \} e^{\hat{T}} | 0 \rangle, \quad (2)$$

where  $|0\rangle$  is the Hartree–Fock, single-determinant, reference wave function and  $\hat{T}$  is the cluster (excitation) operator for the ground state (computed by solving the CCSD amplitude

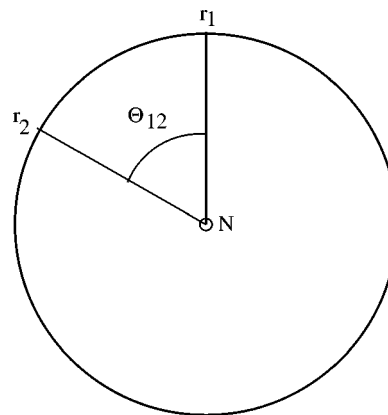


FIG. 1. Schematic diagram of the coordinates used in electron–electron coalescence curve plots. A reference electron is placed at a radius  $r_1$  from the nucleus (at the origin), while the second electron moves in a circle of the same radius containing both the nucleus and electron one.

equations).  $\hat{\Lambda}$ , which is a de-excitation operator analogous to  $\hat{T}$ , parametrizes the left-hand coupled-cluster ground-state wave function. The subscript indices of the annihilation and creation operators refer to molecular spin–orbitals. The two-electron density is perhaps most easily derived using analytic gradient theory, and several authors have presented explicit expressions for the numerous contributions to  $\Gamma^{\text{CCSD}}$  in the literature.<sup>31,33,34</sup>

We have tested the behavior of the two-electron CCSD density as a function of basis set by the following procedure: (1) Select coordinates for each reference electron; (2) compute the basis set representation of Dirac delta functions centered at the chosen coordinates; (3) contract the CCSD two-electron density,  $\Gamma_{pqrs}^{\text{CC}}$ , with the product of the delta functions in the molecular orbital basis. This procedure is equivalent to computing the (coupled cluster) expectation value of the function  $\delta(\mathbf{r}_1, \mathbf{r}_2) = \delta(\mathbf{r}_1) \delta(\mathbf{r}_2)$ , which is related to the simultaneous probability of finding electrons at positions  $\mathbf{r}_1$  and  $\mathbf{r}_2$ . In all calculations reported here, only the correlation contribution to  $\Gamma_{pqrs}^{\text{CC}}$  is computed; we ignore the Hartree–Fock component, which exhibits no cusp behavior regardless of basis set completeness.<sup>35</sup>

We determine the coalescence behavior of the CCSD two-electron density in many-electron atoms by placing one electron a fixed radius,  $r$ , away from the nucleus and moving the second electron in a circle with the same radius with the nucleus at the origin on a plane including the first electron. This scheme is illustrated in Fig. 1. Thus, the angle,  $\theta_{12}$ , between the vectors connecting each electron to the origin serves as a simple coalescence coordinate. In addition, the curvature is computed at  $\theta_{12}=0$  in each case using five-point numerical differentiation.

## III. THE CORRELATION ENERGY VIRIAL RATIO

The quantum-mechanical virial theorem states that, for exact wave functions subject to Coulombic potentials, the expectation values of the kinetic-energy operator,  $\hat{T}$ , and the potential energy operator,  $\hat{V}$ , are related by<sup>36,37</sup>

$$-\frac{\langle V \rangle}{\langle T \rangle} = 2. \quad (3)$$

This ratio also holds for variational wave functions expanded in a complete basis set. For incomplete basis sets, one may scale the functional exponents to force the approximate wave function to satisfy the virial ratio. Lehd and Jensen used this approach to determine the influence of basis set scaling on molecular properties computed using Hartree–Fock self-consistent field (SCF) wave functions.<sup>38</sup> Unfortunately, given the rapid convergence of the SCF method to the CBS limit, the SCF virial ratio showed little sensitivity to the basis set scaling and the observed improvements in molecular properties were minimal.

On the other hand, correlated wave functions, which converge slowly to the CBS limit, could show a greater dependence on basis set scaling, and therefore, the associated virial ratio could prove a more useful diagnostic. Because the total energy is dominated by the Hartree–Fock component, we consider a modified virial ratio involving only the correlation contributions to the kinetic and potential energies. In cases for which the Hartree–Fock virial ratio is already approximately  $-2$ , the CBS “correlated virial ratio” is

$$\frac{\langle V_{\text{corr}} \rangle}{\langle T_{\text{corr}} \rangle} = -2. \quad (4)$$

We have tested the relationship between basis set completeness and the correlation energy virial ratio again using the CCSD approach. We compute the expectation value of the kinetic energy operator by contracting the CCSD one-electron density [using expressions analogous to Eqs. (1) and (2) above] with the kinetic-energy integrals in the molecular orbital basis. Given the total correlation energy, which we must compute in order to obtain the one-electron density, we obtain the potential energy expectation value by subtracting the kinetic-energy component. The one-electron density is well known from analytic gradient theory, and, just as for the two-electron density, explicit equations for its evaluation at the CCSD level appear in the literature.

As noted earlier, a uniform scaling of the primitive Gaussian exponents will enforce the virial ratio even within a finite basis set. As shown originally by Löwdin,<sup>39</sup> such a scaling is tantamount to variational optimization of the total energy with respect to an exponent scale factor,  $\zeta$ . We have applied this optimization procedure to the correlation contribution to the total CCSD energy, which we anticipate to be much more sensitive to basis set scaling than the Hartree–Fock energy.

Strictly speaking, the virial theorem applies only to variational wave functions, such as Hartree–Fock or configuration interaction, for which the computed energy is an upper bound to the exact energy. Coupled cluster wave functions, while size extensive, are not variational, and CCSD energies that fall below the exact (full configuration interaction) result are common in multiconfigurational or quasidegenerate cases (e.g., stretched bonds). However, in each of the atomic cases presented here, the Hartree–Fock reference function is well-behaved, and the coupled cluster wave function is *approximately* variational. In such cases, we may rea-

TABLE I. CCSD correlation virial ratios ( $-V_{\text{corr}}/T_{\text{corr}}$ ) for noble gas atoms for cc-pVXZ and cc-pCVXZ basis sets. Columns labeled “fzc” include only valence electrons.

Basis set	He	Ne	Ne(fzc)	Ar	Ar(fzc)
cc-pVDZ	2.55	-4.10	-5.14	-21.13	4.74
cc-pVTZ	1.99	2.28	1.95	-6.02	2.07
cc-pVQZ	2.01	2.25	2.03	-2.33	2.16
cc-pV5Z	2.00	2.23	2.02	9.57	2.11
cc-pCVDZ	...	5.88	8.29	3.04	2.47
cc-pCVTZ	...	1.98	1.91	2.23	1.93
cc-pCVQZ	...	2.01	1.97	2.10	2.02
cc-pCV5Z	...	2.02	2.00	2.04	2.04

sonably expect coupled cluster wave functions to adhere to the virial theorem, at least within the confines of testing the virial ratio’s relationship to basis set completeness.

#### IV. COMPUTATIONAL DETAILS

Test calculations on the noble gases He, Ne, and Ar, employed the Dunning correlation-consistent basis sets cc-pVXZ and cc-pCVXZ ( $X=D,T,Q,5,6$ ), which include up to  $i$ -type angular momentum functions for Ne and Ar.<sup>9,40</sup> For the calcium atom, we used the  $[6s5p3d]$  and  $[7s7p4d1f]$  ANO contractions of the  $(17s12p4d)$  primitive basis sets developed by Roos and co-workers<sup>41,42</sup> as well as the split-valence 6-311G( $2df,2pd$ ) basis set of Blaudeau *et al.*<sup>43</sup> The ANO basis sets are identical apart from the number of contracted functions included in each and the addition of  $f$ -type functions in the latter.

For closed-shell atoms, all CCSD calculations reported here used spin-restricted Hartree–Fock (RHF) references, while for open-shell species, such as the P atom ( $^4S$ ), we used spin-restricted open-shell Hartree–Fock (ROHF) reference orbitals. In open-shell cases, contributions from the  $\alpha - \alpha, \beta - \beta$ , and  $\alpha - \beta$  two-electron densities were summed, so that the electron coalescence curves and virial components include all spin components. All calculations made use of the PSI3 program package.<sup>44</sup>

#### V. THE NOBLE GASES HELIUM, NEON, AND ARGON

Table I summarizes the correlated virial ratios for the noble-gas atoms as a function of basis set. For the He atom, for which CCSD is equivalent to full CI, the extension of the basis set clearly leads to improvement in the virial ratio towards the exact value of 2, and at the cc-pV6Z level, which includes  $g$ -type functions on He, the ratio is at 2.001 06. For larger atoms with all electrons correlated, however, the trend is less well-behaved, and, with the small cc-pVDZ basis set, the correlated virial ratio for Ne is actually less than zero due to the negative correlation correction for the kinetic energy. This problem is exacerbated for Ar, for which even the large cc-pVQZ basis set gives a negative correlated virial ratio. (The Hartree–Fock ratio for this basis set differs from the ideal 2 only in the eighth decimal place.) However, we note that the cc-pVXZ basis sets were designed to describe correlation among the *valence* electrons only, and when the Ne  $1s$  and Ar  $1s2s2p$  core orbitals are frozen, the CCSD virial ratios improve considerably, as indicated in the Table. To

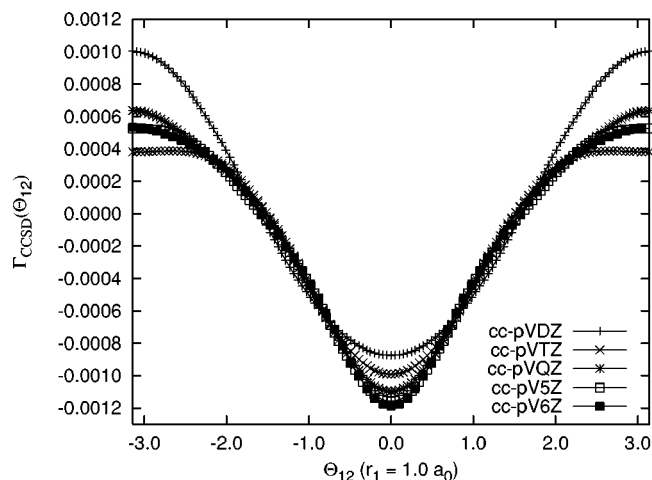


FIG. 2. CCSD electron coalescence plots for He using the cc-pVXZ basis sets.

support this point, Table I also includes virial ratios for the cc-pCVXZ basis sets,<sup>40</sup> which are extensions of the standard cc-pVXZ sets intended to allow for core-core and core-valence correlation. As indicated in the Table, all-electron CCSD calculations with these basis sets show significantly improved correlation virial ratios relative to the cc-pVXZ sets.

Figures 2–4 present plots of the CCSD two-electron density in He, Ne, and Ar, respectively, as a function of  $\Theta_{12}$  for a reference-electron radius of  $1.0 a_0$  and with only valence electrons correlated. In addition, Table II reports the curvature,  $\partial^2\Gamma/\partial\Theta_{12}^2$  at the coalescence point  $\Theta_{12}=0$  for each curve in the Figures. As expected, as the basis set is improved, the curvature at  $r_{12}=0$  increases, and the corresponding plot exhibits greater “cusplike” behavior. We note that the visual improvement in the curves in Figs. 2–4 is substantial between the cc-pVDZ and cc-pVTZ basis sets, but less dramatic between the cc-pV5Z and cc-pV6Z basis sets. On the other hand, the numerical values of the curvature reported in Table II change more consistently, and each increment in basis set completeness provides approximately

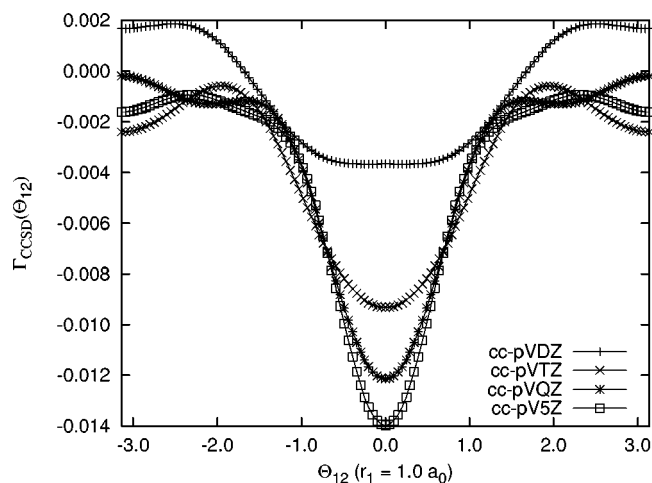


FIG. 3. CCSD electron coalescence plots for Ne with frozen core using the cc-pVXZ basis sets.

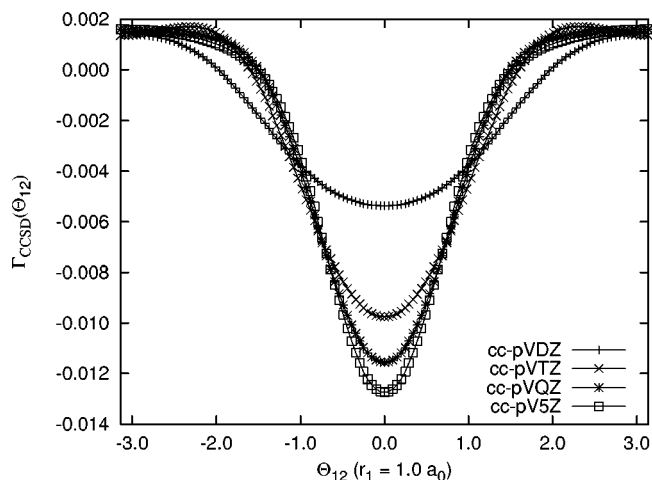


FIG. 4. CCSD electron coalescence plots for Ar with frozen core using the cc-pVXZ basis sets.

the same absolute improvement in  $\partial^2\Gamma/\partial\Theta_{12}^2$ . However the coalescence curvature is clearly a size-extensive quantity, as illustrated by the variation between all-electron and frozen-core curvatures for the Ar atom in Table II. As a result, the diagnostic is useful only for comparing basis set characteristics between calculations involving the same number of correlated electrons.

As mentioned earlier, a uniform scaling of the basis set exponents can force approximate variational wave functions to obey the virial theorem exactly. This is equivalent to optimization of the energy with respect to the scaling value,  $\zeta$ , which plays the role of an additional variational parameter in the model. We have applied this idea to the nonvariational CCSD wave function by numerical optimization of the correlation energy with respect to the scaled primitive Gaussian exponents in the cc-pVXZ basis sets. Figure 5 plots the expectation value of the CCSD kinetic energy and the correlated virial ratio for the He atom with the cc-pVDZ basis set. The optimum scale factor in this case is  $\sim 1.1$ , which changes the total He CCSD energy by only  $-0.000284 E_h$ . Interestingly, for smaller scaled factors (around 0.85), the kinetic-energy contribution to the correlation energy passes through zero, leading to a pole in the virial ratio. Figure 6, which plots the same data for Ar using the cc-pV5Z basis set, shows much more erratic behavior. In this case, the correlation kinetic energy has two singular values as a function of

TABLE II. CCSD electron coalescence curvatures ( $\times 10^4$ ) for noble gas atoms for cc-pVXZ and cc-pCVXZ basis sets. Columns labeled “fzc” include only valence electrons.

Basis set	He	Ne	Ne(fzc)	Ar	Ar(fzc)
cc-pVDZ	7.37	-2.85	-2.94	28.27	26.64
cc-pVTZ	11.79	93.47	93.33	126.52	115.81
cc-pVQZ	16.43	252.93	253.00	220.10	198.49
cc-pV5Z	20.56	383.35	383.77	406.61	276.82
cc-pCVDZ	...	-2.78	-2.95	30.64	28.89
cc-pCVTZ	...	92.58	93.09	134.59	121.77
cc-pCVQZ	...	253.14	253.79	228.49	203.73
cc-pCV5Z	...	382.57	383.38	326.54	287.48

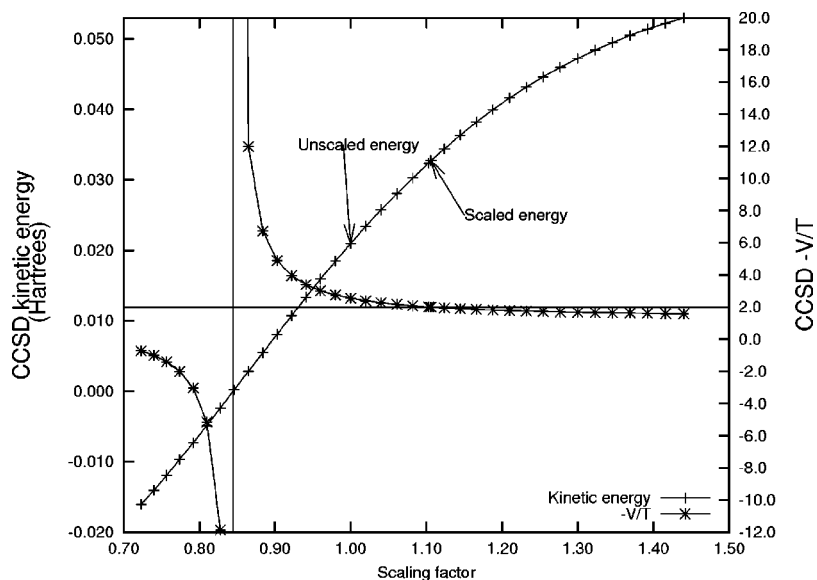


FIG. 5. CCSD kinetic energy (left axis) and CCSD  $-V/T$  (right axis) vs scaling factor for He using cc-pVDZ basis set.

scale factor, at  $\sim 1.10$  and  $1.43$ , thus explaining the large virial ratio for Ar (9.6—cf. Table I) with this basis set. In addition, the optimum scale factor is very large ( $\sim 2.6$ ), which results in dramatic changes in the total CCSD energy for Ar of  $\sim 10\%$ . These observations suggest that basis set scaling in terms of correlation contributions is not reliable. However, further study of this problem is warranted, including separation of scalings for core and valence electron contributions.

## VI. THE CALCIUM ATOM

As noted earlier, flaws in published calcium ANO basis sets led to errors in theoretical predictions of the Ca–O bond length and electronic transition energies in the  $\text{Ca}^+$  atom. Analysis of the basis set structure by Wesolowski *et al.* revealed that the lack of tight  $d$ -type functions caused the errors. Figure 7 shows the electron coalescence plot and Table III summarizes the virial ratio and electron coalescence

curvature data for the  $\text{Ca}^+$  cation for three different basis sets: The 6-311G( $2df,2pd$ ) split-valence set of Blaudeau *et al.*,<sup>43</sup> the  $(17s12p4d)/[6s5p3d]$  and  $(17s12p4d1f)/[7s7p4d1f]$  Roos ANO basis sets,<sup>41,42</sup> and the ANO sets plus a single set of contracted  $d$ -type functions with exponents taken from the Blaudeau basis set  $\alpha_d = 15.08, 3.926, \text{ and } 1.233$ . The ANO basis sets give poor virial ratios and coalescence curvatures relative to the Blaudeau basis set, and the coalescence curves shown in the Figure are dramatically different. The  $(17s12p4d)/[6s5p3d]$  basis set has a negative curvature at  $\Theta_{12}=0$ . The addition of the tight  $d$ -type functions makes a substantial improvement of both the  $(17s12p4d)/[6s5p3d]$  and the  $(17s12p4d1f)/[7s7p4d1f]$  sets, and the difference between the latter and the well-behaved Blaudeau basis set is almost indiscernible. In the case of the calcium atom, the correlation virial ratio and electron coalescence curves appear to be strong comparative indicators of basis set flaws.

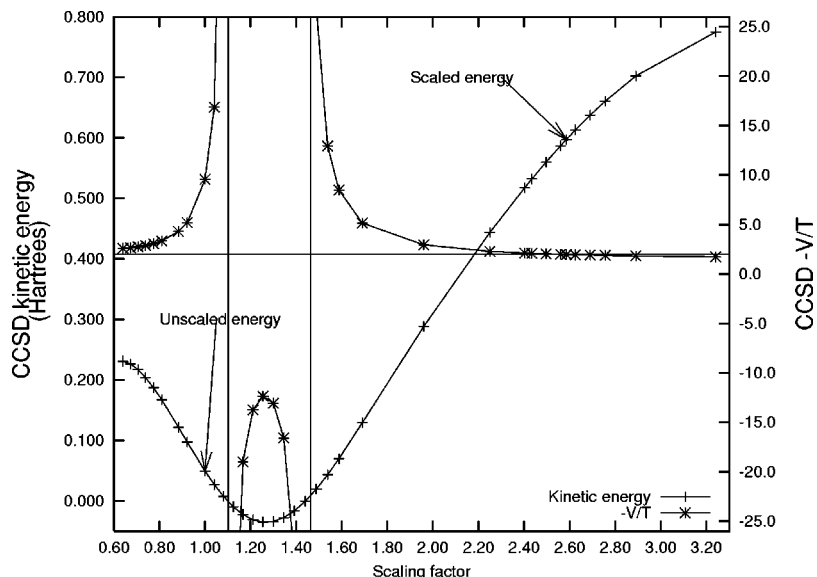


FIG. 6. CCSD kinetic energy and CCSD  $-V/T$  vs scaling factor for Ar using cc-pV5Z basis set.

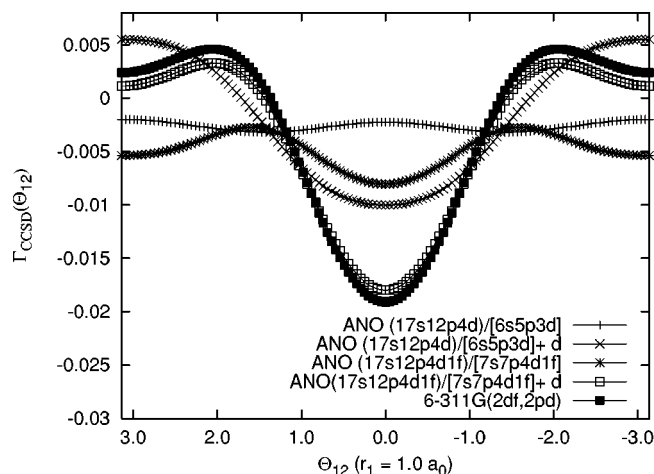


FIG. 7. CCSD electron coalescence plots for  $\text{Ca}^+$  with frozen core using the Roos ANO (Refs. 41 and 42) and Blaudeau *et al.* (Ref. 43) split-valence basis sets.

## VII. THE PHOSPHORUS ATOM

In a number of applications in the last few years, errors observed in the cc-pVXZ basis sets for molecules involving the second-row atoms Al–Ar led to the re-evaluation of the structure of the  $d$  space in these sets. Several authors recognized that one deficiency of the basis sets was the lack of inner-polarization/core functions, resulting in errors of several kcal/mol in binding energies of molecules containing second-row atoms. This deficiency manifested itself primarily in Hartree–Fock contributions to the molecular energies. Both Martin<sup>45</sup> and Bauschlicher and Ricca<sup>46</sup> recommended modifications to the TZ, QZ and 5Z sets to correct the problem. Some time later, Dunning and co-workers provided an additional systematic analysis of the errors, and developed the modified cc-pV(X+d)Z basis sets.<sup>8</sup>

Table IV summarizes valence-only phosphorus-atom CCSD correlation virial ratios and electron coalescence curvatures for the cc-pVXZ and cc-pV(X+d)Z basis sets. The curvatures in this case were computed at a reference radius of  $r = 1.5a_0$ , which is appropriate for the  $d$ -type exponents of  $\sim 3.0$ . As expected, larger basis sets yield higher curvatures and improved virial ratios. However, in this case the addition of high-exponent  $d$ -type functions has relatively little effect on either the coalescence curvatures or the virial ratios, and reasonable results for the latter are obtained with all basis sets. This result is to be expected given the nature of

TABLE III. CCSD correlation virial ratios and electron coalescence curvatures for  $\text{Ca}^+$  including valence electrons only.

Basis set	$-V_{\text{corr}}/T_{\text{corr}}$	Curvature ( $\times 10^4$ )
ANO (17s12p4d)/[6s5p3d] <sup>a</sup>	0.83	-23.55
ANO (17s12p4d)/[6s5p3d]+tight $d$	-1.70	56.08
ANO (17s12p4d1f)/[7s7p4d1f] <sup>b</sup>	0.11	91.81
ANO (17s12p4d1f)/[7s7p4d1f]+tight $d$	2.26	260.35
6-311G(2df,2pd) <sup>c</sup>	2.38	292.64

<sup>a</sup>See Ref. 41.

<sup>b</sup>See Ref. 42.

<sup>c</sup>See Ref. 43.

TABLE IV. CCSD electron coalescence curvatures ( $\times 10^4$ ) for the phosphorus atom ( $^4S$ ) using cc-pVXZ basis sets and including valence electrons only. The “+d” column corresponds to the cc-pV(X+d)Z basis sets (X = D, T, Q, 5) defined by Dunning, Peterson, and Wilson (Ref. 8). Curvatures were determined using a reference radius of  $1.5 a_0$  from the nucleus.

Basis set	cc-pVXZ		cc-pV(X+d)Z	
	Curvature	$-V_{\text{corr}}/T_{\text{corr}}$	Curvature	$-V_{\text{corr}}/T_{\text{corr}}$
DZ	1.65	2.06	1.75	1.91
TZ	4.35	2.04	4.35	2.01
QZ	6.76	2.07	6.79	2.07
5Z	9.31	2.10	9.38	2.10

the basis-set deficiency in this case: Lack of inner-polarization functions in the original second-row cc-pVXZ basis sets is mainly a *molecular* effect, and, as observed by Martin,<sup>45</sup> has the greatest negative impact on the SCF contributions to the energy. Because the basis-set diagnostics examined here are intended to focus on correlation components, they necessarily fail to elucidate the SCF-level errors of the cc-pVXZ basis sets for phosphorus.

## VIII. CONCLUSIONS

We have presented two techniques for measuring the completeness of one-electron basis sets for quantum-chemical calculations: the electron–electron coalescence curve and the correlation virial ratio. The former is based on the Kato cusp condition that exact wave functions should exhibit discontinuous first derivatives with respect to  $r_{12}$  as the coordinates of any two electrons merge. The latter is based on a simple extension of the quantum-mechanical virial theorem focusing on the correlations contributions to the kinetic and potential energy expectation values. We have tested these techniques on a number of atomic systems at the CCSD level of theory and find a strong correlation between the behavior of both the coalescence curves and the virial ratio and the quality of the basis set. The example of the calcium cation, for which published ANO basis sets have exhibited significant shortcomings, is particularly encouraging. On the other hand, the coalescence curves and virial ratio, which are designed to determine errors in the basis set related to electron correlation effects, are insufficiently sensitive to distinguish errors related to Hartree–Fock-level contributions alone, such as those observed in the cc-pVXZ basis sets for the phosphorus atom.

Although it is unlikely that only one or two simple metrics will serve as true diagnostics for all cases, we find that the electron–electron coalescence curves and the correlation virial ratio have strong potential for identifying inadequacies in one-electron basis sets. Our future work in this area will involve: (1) Development of simpler quantification of the electron coalescence curves that, unlike the coalescence curvature, allows comparison between systems with different numbers of electrons; (2) extension of the current analysis to other levels of theory [e.g., MBPT(2) and CCSD(T)]; and (3) extension to molecular test cases.

## ACKNOWLEDGMENTS

This work was supported by a Research Innovation Award from the Research Corporation. The authors would like to thank Dr. Edward F. Valeev (Georgia Tech) for helpful discussions and Dr. Kirk Peterson (Washington State University and Pacific Northwest National Labs) for providing the cc-pCVXZ basis sets for the argon atom prior to their publication.

- <sup>1</sup>R. J. Bartlett, *Annu. Rev. Phys. Chem.* **32**, 359 (1981).
- <sup>2</sup>R. G. Parr and W. Yang, *Density-Functional Theory of Atoms and Molecules* (Oxford University, New York, 1989).
- <sup>3</sup>T. D. Crawford and H. F. Schaefer, in *Reviews in Computational Chemistry*, edited by K. B. Lipkowitz and D. B. Boyd (VCH, New York, 2000), Vol. 14, Chap. 2, pp. 33–136.
- <sup>4</sup>R. J. Bartlett, in *Modern Electronic Structure Theory*, Vol. 2 of *Advanced Series in Physical Chemistry*, edited by D. R. Yarkony (World Scientific, Singapore, 1995), Chap. 16, pp. 1047–1131.
- <sup>5</sup>T. J. Lee and G. E. Scuseria, in *Quantum Mechanical Electronic Structure Calculations With Chemical Accuracy*, edited by S. R. Langhoff (Kluwer, Dordrecht, 1995), pp. 47–108.
- <sup>6</sup>J. Almlöf, T. Helgaker, and P. R. Taylor, *J. Phys. Chem.* **92**, 3029 (1988).
- <sup>7</sup>J. Almlöf and P. R. Taylor, *J. Chem. Phys.* **86**, 4070 (1987).
- <sup>8</sup>T. H. Dunning, K. A. Peterson, and A. K. Wilson, *J. Chem. Phys.* **114**, 9244 (2001).
- <sup>9</sup>T. H. Dunning, *J. Chem. Phys.* **90**, 1007 (1989).
- <sup>10</sup>L. A. Curtiss, K. Raghavachari, G. W. Trucks, and J. A. Pople, *J. Chem. Phys.* **94**, 7221 (1991).
- <sup>11</sup>L. A. Curtiss, K. Raghavachari, P. C. Redfern, V. Rassolov, and J. A. Pople, *J. Chem. Phys.* **109**, 7764 (1998).
- <sup>12</sup>M. R. Nyden and G. A. Petersson, *J. Chem. Phys.* **75**, 1843 (1981).
- <sup>13</sup>G. A. Petersson and S. L. Licht, *J. Chem. Phys.* **75**, 4556 (1981).
- <sup>14</sup>A. G. Császár, W. D. Allen, and H. F. Schaefer, *J. Chem. Phys.* **108**, 9751 (1998).
- <sup>15</sup>S. S. Wesolowski, E. F. Valeev, R. A. King, V. Baranovski, and H. F. Schaefer, *Mol. Phys.* **98**, 1227 (2000).
- <sup>16</sup>K. Raghavachari, G. W. Trucks, J. A. Pople, and M. Head-Gordon, *Chem. Phys. Lett.* **157**, 479 (1989).
- <sup>17</sup>J. F. Stanton and R. J. Bartlett, *J. Chem. Phys.* **98**, 7029 (1993).
- <sup>18</sup>D. P. Chong and S. R. Langhoff, *J. Chem. Phys.* **93**, 570 (1990).
- <sup>19</sup>D. P. Chong, *Can. J. Chem.* **73**, 79 (1995).
- <sup>20</sup>A. A. Auer, T. Helgaker, and W. Klopper, *J. Comput. Chem.* **23**, 420 (2002).
- <sup>21</sup>T. Kato, *Commun. Pure Appl. Math.* **10**, 151 (1957).
- <sup>22</sup>W. Klopper and W. Kutzelnigg, *Chem. Phys. Lett.* **134**, 17 (1987).
- <sup>23</sup>W. Kutzelnigg and W. Klopper, *J. Chem. Phys.* **94**, 1985 (1990).
- <sup>24</sup>J. Noga and W. Kutzelnigg, *J. Chem. Phys.* **101**, 7738 (1994).
- <sup>25</sup>W. Klopper, *r<sub>12</sub>-dependent wave functions*, 1996, Habilitationsschrift, Eidgenössischen Technischen Hochschule Zürich.
- <sup>26</sup>E. F. Valeev and H. F. Schaefer, *J. Chem. Phys.* **113**, 3990 (2000).
- <sup>27</sup>E. F. Valeev, W. D. Allen, H. F. Schaefer, and A. G. Császár, *J. Chem. Phys.* **114**, 2875 (2002).
- <sup>28</sup>E. R. Davidson, in *Reduced Density Matrices in Quantum Chemistry* (Academic, New York, 1976), pp. 103–104.
- <sup>29</sup>G. D. Purvis and R. J. Bartlett, *J. Chem. Phys.* **76**, 1910 (1982).
- <sup>30</sup>R. J. Bartlett, in *Geometrical Derivatives of Energy Surfaces and Molecular Properties*, edited by P. Jørgensen and J. Simons (Reidel, Dordrecht, 1986), pp. 35–61.
- <sup>31</sup>A. C. Scheiner, G. E. Scuseria, J. E. Rice, T. J. Lee, and H. F. Schaefer, *J. Chem. Phys.* **87**, 5361 (1987).
- <sup>32</sup>E. A. Salter, G. W. Trucks, and R. J. Bartlett, *J. Chem. Phys.* **90**, 1752 (1989).
- <sup>33</sup>J. Gauss, J. F. Stanton, and R. J. Bartlett, *J. Chem. Phys.* **95**, 2623 (1991).
- <sup>34</sup>J. Gauss and J. F. Stanton, *J. Chem. Phys.* **103**, 3561 (1995).
- <sup>35</sup>T. Helgaker, P. Jørgensen, and J. Olsen, *Molecular Electronic-Structure Theory* (Wiley, New York, 2000).
- <sup>36</sup>E. Merzbacher, *Quantum Mechanics*, 2nd ed. (Wiley, New York, 1970).
- <sup>37</sup>F. L. Pilar, *Elementary Quantum Chemistry*, 2nd ed. (McGraw-Hill, New York, 1990).
- <sup>38</sup>M. Lehd and F. Jensen, *J. Comput. Chem.* **12**, 1089 (1991).
- <sup>39</sup>P. Löwdin, *J. Mol. Spectrosc.* **3**, 46 (1959).
- <sup>40</sup>D. E. Woon and T. H. Dunning, *J. Chem. Phys.* **103**, 4572 (1995).
- <sup>41</sup>P.-O. Widmark, B. Persson, and B. Roos, *Theor. Chim. Acta* **79**, 419 (1991).
- <sup>42</sup>K. Pierloot, B. Dumez, P. Widmark, and B. O. Roos, *Theor. Chim. Acta* **90**, 87 (1995).
- <sup>43</sup>J.-P. Blaudeau, M. P. McGrath, L. A. Curtiss, and L. Radom, *J. Chem. Phys.* **107**, 5016 (1997).
- <sup>44</sup>PSI3.0., T. D. Crawford, C. D. Sherril, E. F. Valeev *et al.*
- <sup>45</sup>J. M. L. Martin, *J. Chem. Phys.* **108**, 2791 (1998).
- <sup>46</sup>C. W. Bauschlicher and A. Ricca, *J. Phys. Chem. A* **102**, 8044 (1998).